An Ultrawideband Ultrathin Metamaterial Absorber Based on Circular Split Rings

Saptarshi Ghosh, *Student Member, IEEE*, Somak Bhattacharyya, *Student Member, IEEE*, Devkinandan Chaurasiya, and Kumar Vaibhav Srivastava, *Senior Member, IEEE*

***Abstract*—A simple design model for making ultrawideband ultrathin metamaterial absorber has been presented in microwave frequency regime. The proposed structure is composed of two concentric circular split rings imprinted on a metal-backed dielectric substrate. A 10-dB absorption bandwidth from 7.85 to 12.25 GHz covering the entire X-band has been observed in numerical simulation under normal incidence. The absorptivities of the proposed structure have been investigated under different polarization angles as well as oblique incidence. The electromagnetic field distributions and surface current plots have been illustrated to analyze the absorption mechanism of the proposed structure. The proposed absorber has been fabricated and its performance is experimentally verified at different angles of incidence and polarizations of incident electromagnetic wave. The designed absorber is compact, ultrathin (only $\lambda_0/15$ thick corresponding to center frequency) and provides an alternative to construct broadband absorber for many potential applications.**

***Index Terms*—Broadband absorber, circular split ring, metamaterial, microwave absorber.**

I. Introduction

ELECTROMAGNETIC metamaterials (MTM) [1] are artificial composite structures, which can attain its properties from the unit cell structure. Due to their attractive properties in sub-wavelength scale, metamaterials are nowadays experimentally used in many applications like perfect lens [2], antenna [3], cloaking [4], and so forth. Metamaterial-based absorbers can be used as potential alternatives of conventional absorbers due to their ultrathin thickness, near unity absorption properties, simple manufacturing procedures, and increasing effectiveness [5], [6].

These metamaterial absorber structures are generally composed of a periodic array of top metallic patch and ground metal plane separated by dielectric substrate. At resonance frequency, the top frequency selective surface (FSS) is electrically excited, whereas the incident magnetic field excites the dielectric substrate forming circulating flow of surface current. These electromagnetic fields can simultaneously manipulate the effective material properties of the homogenized structure, such that the effective permittivity and effective permeability of the structure become equal to each other at certain frequencies [5]. This results the input impedance of the structure to match closely with the free space impedance of air, thereby reducing the reflection from the absorber structure.

Despite ultrathin nature and near-unity absorption, the metamaterial absorbers suffer from narrow operating bandwidth as they are designed using resonance phenomenon [5]. Some single layer bandwidth-enhanced absorber structures have been presented with moderate bandwidths [7], [8]. However, their patterns are complicated, and it is difficult to simultaneously control each resonant frequency of such multiresonant structures. Another approach for a broadband absorber is by combining two or more different resonant structures to form a new resonator [9], [10]. Although this type of absorber exhibits bandwidth-enhanced absorption with simpler structure geometry, the unit cell dimensions are too large to implement them in practical applications. Some absorber designs also comprise multiple vertically stacked metallic layers, but the thickness is also a major limitation in those designs [11]–[13].

In this letter, a novel ultrawideband ultrathin metamaterial absorber has been proposed, which exhibits above 90% absorption bandwidth for the frequency range of 7.85–12.25 GHz. Two circular split rings have been embedded one inside another, where the outer ring provides dual-band absorption and the bandwidth is considerably increased by the inner one. The electromagnetic field distributions and the surface current plots at the absorption peaks have been illustrated to analyze the absorption mechanism of the broadband absorber. The designed structure has been studied for different angles of polarization under normal incidence as well as for wide incident angles. The radii as well as the rotational angles of the splits of the circular rings have been varied to observe their contributions to the broadband absorption. The structure has been fabricated using printed circuit board (PCB) technology and the experimental results are in good agreement with the simulated responses. Compared to the metamaterial absorbers presented before, the proposed absorber has the advantages of ultrathin nature ($\sim \lambda_0/15$), miniaturization, ultrawideband coverage as well as experimental verification.

II. Design and Simulated Results

Fig. 1 shows the design of the proposed broadband absorber. The single unit cell consists of a top metallic patch and bottom ground plane separated by dielectric substrate. FR-4 substrate (relative permittivity $\varepsilon_r = 4.2$ and dielectric loss tangent

Manuscript received November 15, 2014; accepted January 19, 2015. Date of publication January 23, 2015; date of current version May 22, 2015. This work was supported in part by DRDO, India, under Project No. DLJ/TC/1025/I/30 and ISRO-IITK Space Technology Cell under Project No. STC/EE/2014087.

The authors are with the Department of Electrical Engineering, Indian Institute of Technology Kanpur, Uttar Pradesh 208016, India (e-mail: joysaptarshi@gmail.com; bhattacharyya.somak@gmail.com; chaurasiya.dev1189@gmail.com; kvs@iitk.ac.in).

Color versions of one or more of the figures in this letter are available online at http://ieeexplore.ieee.org.

Digital Object Identifier 10.1109/LAWP.2015.2396302

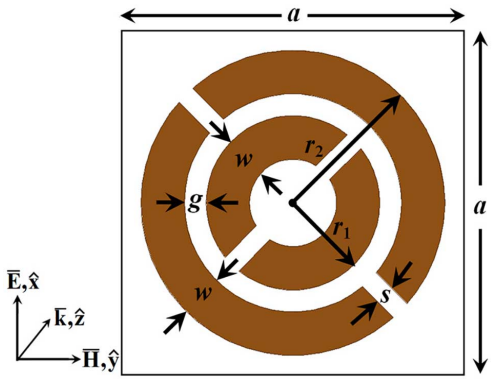

Fig. 1. Front view of the proposed ultrawideband ultrathin unit cell structure with geometrical dimensions: $a = 7.1$, $r_1 = 1.8$, $r_2 = 3.15$, $w = 0.9$, $g = 0.45$, $s = 0.4$ (unit: mm).

$tan\ \delta = 0.02$) has been used as dielectric with thickness of 2 mm. The top layer is constituted of two concentric circular rings with each ring having two splits. The splits are oriented in orthogonal positions along the diagonals of the unit cell structure. Both the top patch and bottom ground are made of copper with conductivity $\sigma = 5.8 \times 10^7$ S/m and a thickness of 0.035 mm. The dimensions of the unit cell along with the directions of field vectors are shown in Fig. 1.

In order to analyze an infinite array of the proposed absorber, the unit cell is simulated with periodic boundary conditions using ANSYS HFSS. The absorptivity (A) can be expressed as: $A = 1 - |S_{11}|^2 - |S_{21}|^2$, where $|S_{11}|^2$ is the reflected power and $|S_{21}|^2$ is the transmitted power. Since the back side is covered with metal plane, there is no transmission ($|S_{21}|^2 = 0$). Therefore, the absorptivity can be obtained by minimizing the reflectance from the absorber structure. It is observed from Fig. 2(a) that the reflection coefficient is less than -10 dB in the entire X-band (8–12 GHz), and the absorption bandwidth above 90% ranges from 7.85 to 12.25 GHz, which is 44% at 10 GHz. The two absorption peaks are also visible at 8.36 and 11.18 GHz with absorptivities of 99.66% and 99.92%, respectively.

In order to demonstrate the polarization behavior of the broadband absorber, the structure has been studied under different polarization angles from 0° to 90° in the steps of 15°, as shown in Fig. 2(b). The simulated absorptivity plot shows that the proposed structure is two-fold symmetric, i.e. the absorptivity gradually decreases with higher polarization angles, reaches minimum at 45°, an then again increases to end up at maximum absorption for 90° polarization angle. The proposed absorber has also been examined for different incident angles (upto 45°) under TE polarization as shown in Fig. 2(c). It is seen that with increasing oblique incident angle, the broadband absorption response gradually changes to dual-band absorption.

III. Absorption Mechanism

In order to gain a better insight about the absorption mechanism, the electric and magnetic field distributions have been illustrated in Fig. 3 at the two absorption peaks, viz. 8.36 and 11.18 GHz. Analyzing the results, it is clearly observed that at the lower resonance of around 8.36 GHz, the outer circular ring is the primary contributor and provides a highly localized electromagnetic field around the ring. At the higher frequency 11.18 GHz, the outer ring also contributes highly, although the inner circular ring has a small contribution at this frequency.

The top and bottom surface current distributions at the peak absorption frequencies 8.36 and 11.18 GHz have also been shown in Fig. 4 and Fig. 5. It clearly depicts that in both the absorption frequencies, the surface current is mainly distributed in the outer circular ring, while a small amount of current flows through the inner ring at the higher frequency. In both the absorption peaks, these surface currents form circulating loops around the incident magnetic field, thereby forming strong magnetic resonance. The electric resonance is coupled with the top metallic patch at these absorption frequencies and high absorption has been realized.

To observe the contribution of the two rings in the absorption bandwidth, the radius of a single circular split ring has been varied from 1.8 mm (equal to inner ring radius of the proposed structure) to 3.15 mm (equal to outer ring radius of the proposed structure) as shown in Fig. 6(a). It is observed that a single circular ring with the splits having radius of 3.15 mm provides two absorption peaks at 8.12 and 12.39 GHz, with a bandwidth of 6.36 GHz (7.58–13.94 GHz) above 80% absorption. On the contrary, the circular split ring with radius of 1.8 mm gives rise to two absorption peaks having 51.34% and 97.98% absorptivities at 17.21 and 24.08 GHz, respectively, with a 50% absorption bandwidth of 10.18 GHz. Since the absorption peaks due to the individual split rings are well apart from each other, there is minor change in absorption frequencies of the outer ring when the inner ring is embedded inside. The two absorption peaks at 8.12 and 12.39 GHz due to the sole outer ring have been shifted to 8.36 and 11.18 GHz, respectively, in the proposed structure due to mutual coupling. Since both the peaks come closer, the minimum absorption in the intermediate frequency range increases, thereby satisfying 90% absorption bandwidth for the entire 7.85–12.25 GHz frequency range. Thus, it is clearly understood that the two absorption peaks of the proposed absorber structure is solely provided by the outer circular ring, whereas the overall absorption bandwidth has been effectively controlled by the inner circular ring.

Another critical parameter to discuss is the effects of rotation of the splits of the inner ring with respect to the outer ring and vice-versa. When the inner circular ring has been rotated keeping the outer ring fixed, the lower absorption peak (which is solely controlled by the outer ring) remains unchanged, whereas the higher absorption peak starts decreasing as shown in Fig. 6(b). On the other hand, Fig. 6(c) shows the rotation of outer circular split ring keeping the inner ring fixed. Since the outer ring controls both the absorption peaks, with changing the angle (ψ_2), both the absorption peaks start deviating and they become minimum and maximum at an angle of 45° and 90°, respectively.

IV. Fabrication and Experimental Results

In order to experimentally demonstrate the proposed absorber, a prototype consisting of 33×33 unit cells, as shown in Fig. 7(a), has been fabricated on a 2 mm thick FR-4 substrate using printed circuit board (PCB) technology. An enlarged portion of the fabricated structure is shown in Fig. 7(b). To measure its reflection spectra, two linearly polarized horn

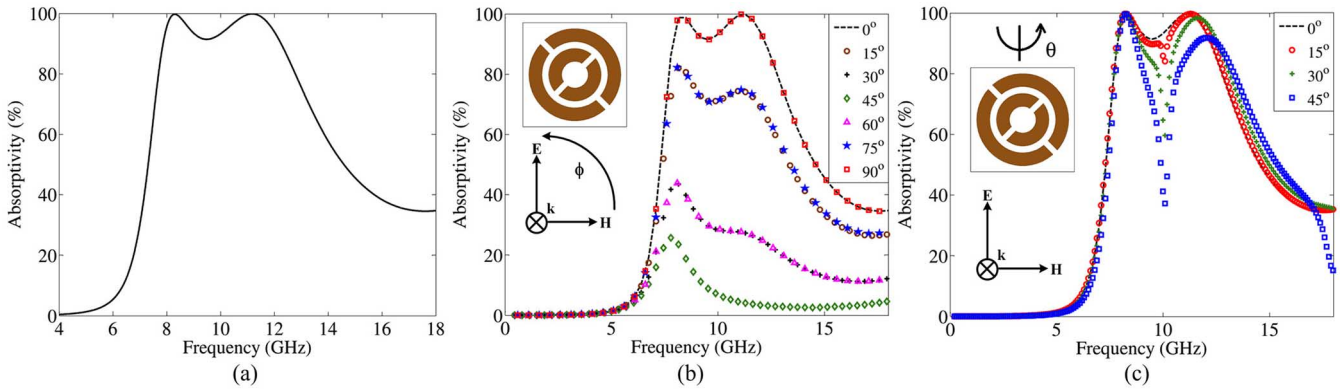

Fig. 2. Simulated absorptivity (a) under normal incidence, (b) for different polarization angles (ϕ) under normal incidence, and (c) for different incidence angles (θ) under TE polarization of the proposed structure.

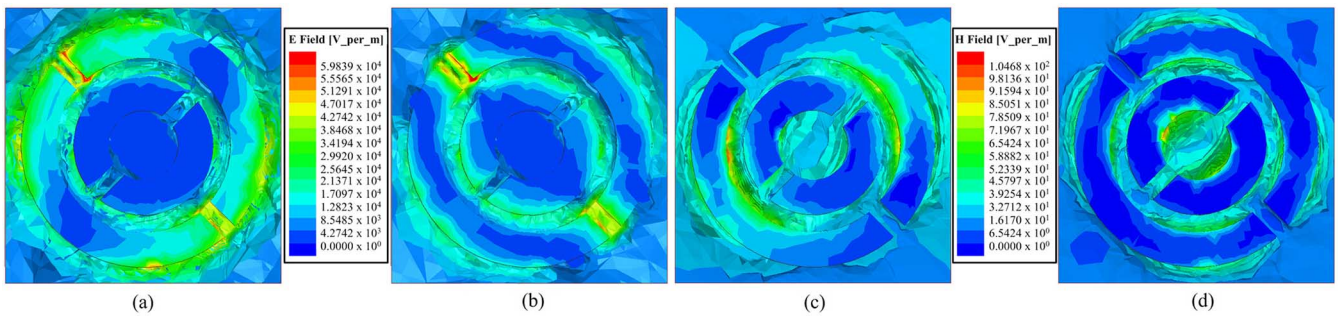

Fig. 3. Simulated electric field distribution at (a) 8.36 and (b) 11.18 GHz and magnetic field distribution at (c) 8.36 and (d) 11.18 GHz of the proposed absorber structure.

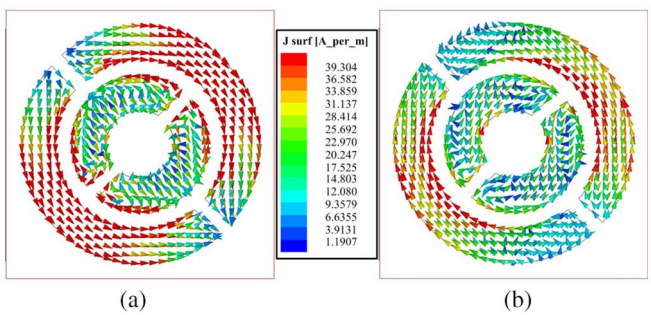

Fig. 4. Surface current distribution on top surface at (a) 8.36 and (b) 11.18 GHz of the proposed structure.

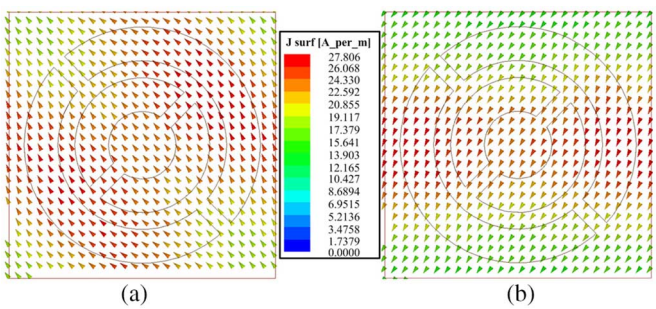

Fig. 5. Surface current distribution on bottom surface at (a) 8.36 and (b) 11.18 GHz of the proposed structure.

antennas (LB-10180-SF), with operating bandwidth from 1 to 18 GHz, have been used to transmit and receive the electromagnetic waves. The network analyzer used for measurements is Agilent Technologies N5230 A with 10 MHz to 50 GHz frequency range.

Initially, a copper sheet of identical dimension has been placed in the anechoic chamber and the reflection coefficient from the plate has been used to calibrate the test environment. The reflection from the fabricated structure is then measured and the difference between the two measured results gives rise to the actual reflection from the fabricated absorber structure. In Fig. 7(c), the measured absorptivity is compared with the simulated response. The measured 10-dB bandwidth is 4.04 GHz from 8.08 to 12.12 GHz, which matches very well with the simulated results. A slight deviation between the simulated and measured results can be explained due to the fabrication tolerance and nonlinear behavior of the dielectric substrate at higher frequencies.

To investigate the polarization-dependence of the proposed absorber, the fabricated structure has been rotated around its axis (from 0° to 90°), and the measured absorptivity response is shown in Fig. 8(a). The measured result exhibits almost same absorption bandwidth for 0° and 90° polarization angles, whereas the absorptivity is decreased to minimum at 45° polarization. Fig. 8(b) shows the measured absorptivities for different incident angles under TE polarization. It is evident from Fig. 8(b) that at higher incident angles the broadband absorption gradually changes to dual-band response, which has good agreement with the simulated results.

V. Conclusion

An ultrawideband ultrathin ($\lambda_0/15$ thick corresponding to free space wavelength and $\lambda_g/7.3$ thick with respect to FR-4 dielectric at the center frequency) metamaterial-based X-band absorber has been presented with two concentric circular split

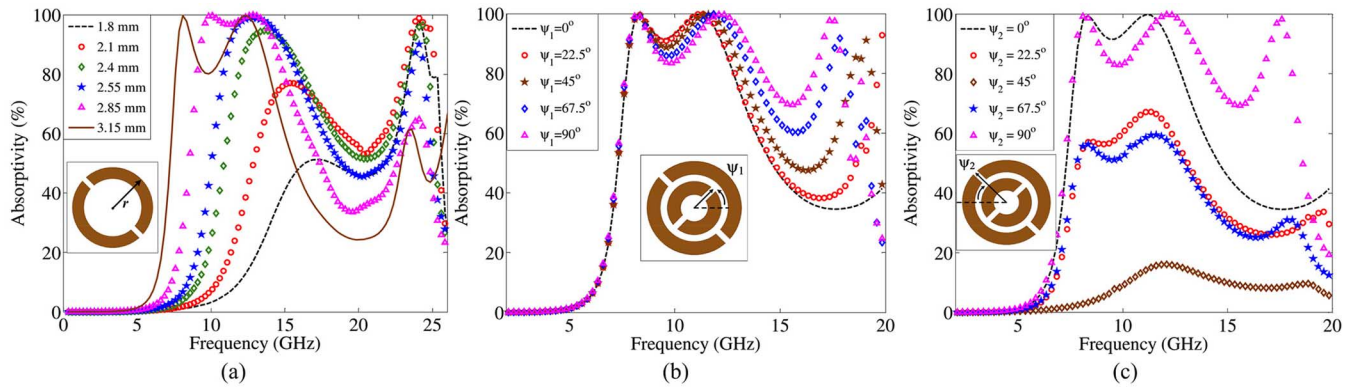

Fig. 6. Simulated absorptivity (a) for different radii of a single circular split ring. Absorptivity of the proposed structure for different rotational angles of the (b) inner circular ring keeping outer ring fixed and (c) outer circular ring with inner ring fixed.

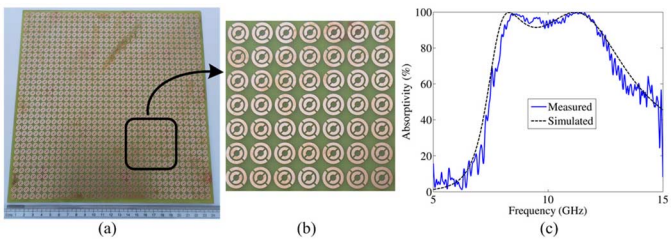

Fig. 7. (a) Fabricated broadband structure, (b) its enlarged view, and (c) comparison of simulated and measured absorptivity under normal incidence.

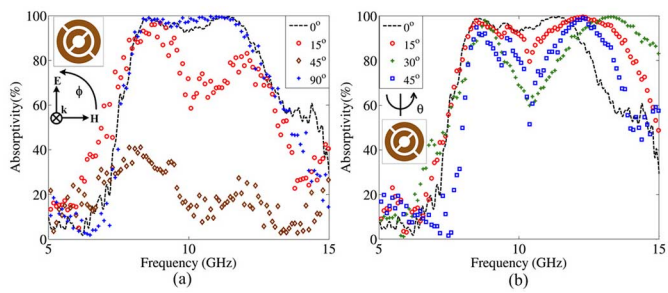

Fig. 8. Measured absorptivity for (a) different polarization angles under normal incidence, and (b) different incident angles under TE polarization of the proposed structure.

TABLE I

Absorber	Centre frequency (GHz)	Unit cell size (mm)	Thickness (mm)	FWHM	Polarization insensitive
Lee et al [7]	10	14.2	0.6 ($0.02\lambda_0$)	11%	Yes
Ghosh et al [8]	9.98	7.2	1 ($0.033\lambda_0$)	11.52%	Yes
Liu et al [9]	11.11	40	0.8 ($0.029\lambda_0$)	20%	Yes
Xiong et al [13]	15.13	6.4	3.65 ($0.18\lambda_0$)	95.2%	No
Yoo et al [14]	10.15	13.8	5.6 ($0.19\lambda_0$)	45% (10 dB)	Yes
Proposed structure	10.05	7.1	2 ($0.067\lambda_0$)	72.64% (43% at -10 dB)	No

rings. The numerical simulation shows above 90% absorption for frequency range of 7.85–12.25 GHz, which is in good agreement with the experimental results. The physical mechanism of absorption using electromagnetic field distributions and surface current plots has been illustrated. The absorption characteristics under different polarization angles as well as oblique incident angles have been studied. The proposed structure has been compared with previously proposed absorbers in Table I and it is clearly observed that the bandwidth of the proposed structure has been significantly increased as compared to [7], [8], and [9]. Although [13] and [14] have higher FWHMs compared to the proposed structure, but their thicknesses are very large. Therefore, the proposed structure is a good alternative of other broadband absorbers and can be used for many potential applications such as stealth technology, electromagnetic interference (EMI), electromagnetic compatibility (EMC) and phase imaging.

REFERENCES

[1] D. R. Smith, W. J. Padilla, D. C. Vier, S. C. Nemat-Nasser, and S. Schultz, "Composite medium with simultaneously negative permeability and permittivity," *Phys. Rev. Lett.*, vol. 84, pp. 4184–4187, 2000.

[2] N. Fang, H. Lee, C. Sun, and X. Zhang, "Sub-diffraction-limited optical imaging with a silver superlens," *Science*, vol. 308, pp. 534–537, 2005.

[3] S. Enoch, G. Tayeb, and P. Vincent, "A metamaterial for directive emission," *Phys. Rev. Lett.*, vol. 89, pp. 3901–3904, 2002.

[4] D. Schurig, J. J. Mock, B. J. Justice, S. A. Cummer, J. B. Pendry, A. F. Starr, and D. R. Smith, "Metamaterial electromagnetic cloak at microwave frequencies," *Science*, vol. 314, pp. 977–980, 2006.

[5] N. I. Landy, S. Sajuyigbe, J. J. Mock, D. R. Smith, and W. J. Padilla, "Perfect metamaterial absorber," *Phys. Rev. Lett.*, vol. 100, p. 207402, 2008.

[6] P. Saville, *Review of Radar Absorbing Materials.* Defense R & D Canada-Atlantic, 2005, pp. 5–15.

[7] J. Lee and S. Lim, "Bandwidth-enhanced and polarization-insensitive metamaterial absorber using double resonance," *Electron. Lett.*, vol. 47, no. 1, pp. 8–9, 2011.

[8] S. Ghosh, S. Bhattacharyya, Y. Kaiprath, and K. V. Srivastava, "Bandwidth-enhanced polarization-insensitive microwave metamaterial absorber and its equivalent circuit model," *J. Appl. Phys.*, vol. 115, p. 104503, 2014.

[9] Y. Liu, S. Gu, C. Luo, and X. Zhao, "Ultra-thin broadband metamaterial absorber," *Appl. Phys. A*, vol. 108, no. 1, pp. 19–24, 2012.

[10] S. Bhattacharyya, S. Ghosh, and K. V. Srivastava, "Triple band polarization-independent metamaterial absorber with bandwidth enhancement at X-band," *J. Appl. Phys.*, vol. 114, p. 094514, 2013.

[11] J. Sun, L. Liu, G. Dong, and J. Zhou, "An extremely broad band material absorber based on destructive interference," *Opt. Exp.*, vol. 19, p. 21155, 2011.

[12] H. Jaradat and A. Akyurtlu, "Infrared (IR) absorber based on multiresonant structure," *IEEE Trans. Antennas Wireless Propag. Lett.*, vol. 11, pp. 1222–1225, 2012.

[13] H. Xiong, J.-S. Hong, C.-M. Luo, and L.-L. Zhong, "An ultrathin and broadband metamaterial absorber using multi-layer structures," *J. Appl. Phys.*, vol. 114, p. 064109, 2013.

[14] M. Yoo and S. Lim, "Polarization-independent and ultrawideband metamaterial absorber using a hexagonal artificial impedance surface and a resistor-capacitor layer," *IEEE Trans. Antennas Propag.*, vol. 62, no. 5, pp. 2652–2658, May 2014.